International Refrigeration and Air Conditioning Conference

School of Mechanical Engineering

2022

Review of Triply Periodic Minimal Surface (TPMS) based Heat Exchanger Designs

Lalith Kannah Dharmalingam

Vikrant Aute

Jiazhen Ling

Review of Triply Periodic Minimal Surface (TPMS) based Heat Exchanger Designs

Lalith Kannah DHARMALINGAM[1], Vikrant AUTE[2]*, Jiazhen LING[3,4]

[1,2,3]Center for Environmental Energy Engineering,
Department of Mechanical Engineering, University of Maryland
College Park, MD 20742 USA
Email: [1]lalithkd@umd.edu, [2]vikrant@umd.edu, [3]jiazhen@umd.edu

[4]National Renewable Energy Laboratory,
Golden, CO 80401 USA
Email: [4]jiazhen.ling@nrel.gov

* Corresponding Author

ABSTRACT

Heat exchangers (HX) are key components in the heating, cooling, and power systems and improving their heat transfer performance has a direct impact on the system efficiencies and global energy sustainability. Conventionally, heat transfer is enhanced by the use of extended secondary surfaces such as baffles in shell based HX, and corrugations in plate-fin HX. These diffusive material structures increase the overall heat transfer area as well as prevent the growth of boundary layer. With increasing sophistications in manufacturing techniques, more compact HX designs with small diameter flow paths and complex flow channels as in the case of printed circuit heat exchangers were made possible. However, these designs have been shown to suffer significant pressure-drop penalties. Rapid growth in the field of additive manufacturing has set off a stream of research into complex shapes and geometries for engineering applications. Triply Periodic Minimal Surfaces (TPMS) are a class of differential surfaces that are gaining such increased interest in the past few years, especially for heat transfer applications. This paper summarizes a comprehensive literature review investigating the use of TPMS structures for HX applications that have been shown to produce 15 – 120% higher heat transfer coefficients for a given pumping power than a printed circuit HX design. Further, three understudied Fisher-Koch (FK) TPMS structures were identified and computationally analyzed for thermal-hydraulic performance to compare with the established superiority of Schwarz-D TPMS structure. The FK TPMS HX designs exhibited 23% - 356% increase in heat transfer while maintaining similar pressure drops when compared to the Schwarz-D TPMS HX design. This paper concludes by identifying key research directions to characterize the thermal-hydraulic performance of TPMS HX designs and their experimental validation.

Keywords: heat exchanger, triply periodic minimal surface, tpms, design

1. INTRODUCTION

Global energy consumption has been increasing by 2%/year until the pandemic in 2019 (Enerdata, 2021) and the trend is expected to continue now that the world is recovering to normalcy. However, according to International Energy Agency (IEA), energy intensity improvement had seen a drop to 1.5% in 2018 from over 2% in the previous years. It is well below the target value of 4%/year over the next 20 years for global sustainability (Motherway, 2020). Hence, it is paramount to improve energy efficiency to ensure global energy sustainability. Heat exchangers are key components in the heating, cooling and power systems used in all industries. Thus, improving the heat transfer effectiveness of Heat eXchangers (HX) directly plays a crucial role in global energy sustainability.

Compact HXs have been an ongoing topic of research for the past few decades and Li et al. (2011) provide a review of different compact HX designs in their work. Most compact HX designs use small characteristic flow diameters, louvered fins and complex flow channels to increase their effective heat transfer area. Along the same line, unstructured metal foams (Lu et al., 2006; Mahjoob and Vafai, 2008) and structured periodic lattices (Ekade and

Krishnan, 2019; Maloney et al., 2012; Pelanconi et al., 2021) have also been investigated for HX designs due to their highly compact structure. Typically, these designs require unconventional manufacturing techniques like special brazing technique for small characteristic diameter tubes and photochemical etching process for complex printed circuit HX designs which hinders their commercialization. However, with the exponential growth in additive manufacturing techniques in the recent decade, it is now possible to realize these complex compact HX designs without the limitations of conventional manufacturing techniques.

Triply Periodic Minimal Surfaces (TPMSs) are a type of periodic structure that are gaining interest in many engineering applications, including HX applications, due to the advancements in additive manufacturing. They are a class of differential surfaces called minimal surfaces. These surfaces are of particular interest since they can pack relatively large surface area in a given volume. In addition, their continuous flexures without sharp edges mean these structures do not have concentration points that can compromise material properties. Their continuous curvature can also reduce the pressure drop penalties that are inherent in other compact HX designs discussed above. The main objective of this work is to identify and characterize thermal-hydraulic performance of different TPMS structures as heat exchangers.

A minimal surface is a differential surface that locally minimizes its surface energy. The simplest minimal surface is the catenoid, discovered by Euler in 1744. It can be realized using a soap film as shown in Figure 1. Mathematically, Meusnier defined minimal surfaces as those with zero mean curvature everywhere and also discovered helicoid as the second minimal surface (Hyde et al., 1996; Meeks and Pérez, 2012). It was not until German professor Hermann Schwarz (1972) who used complex analysis and Weierstraß formula, more complex minimal surfaces were identified. Later, Schoen (1970) named these surfaces in his report where he also identified several new examples of periodic minimal surfaces.
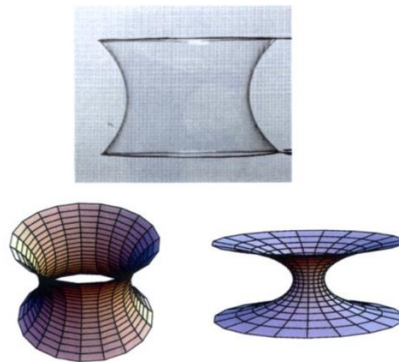

Figure 1: (Top): A region of the catenoid formed by a soap film. (Bottom left): Computer-graphics image of a portion of a catenoid. (Bottom right): larger view showing "trumpet" ends (Hyde et al., 1996)
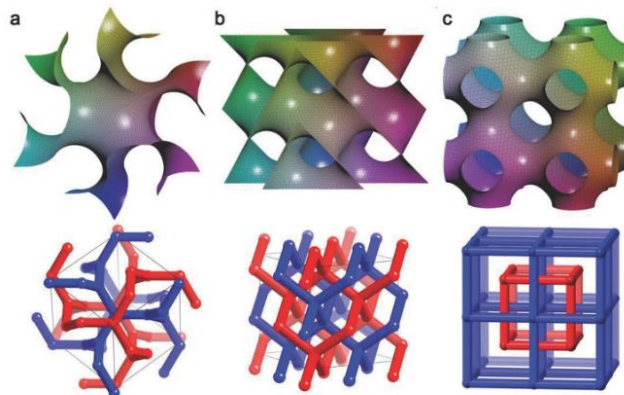

Figure 2: TPMS surfaces and their bi-continuous skeletal graphs: a) Gyroid (G) surface, b) Diamond (D) surface, c) Primitive (P) surface (Han and Che, 2018)

Geometrically, Schwarz minimal surfaces are categorized as genus-3 bi-continuous triply periodic minimal surfaces. That is to say, they have three holes in the surface and divide the three-dimensional Euclidian space into two equal, interpenetrating, intersection-free, infinitely repeating labyrinths. It is this property that makes these surfaces an interesting alternative to traditional HX designs. Alan Schoen named these surfaces based on the crystal lattice they represent as shown in Figure 2. Skeletal graphs representing the crystal lattice with a network of rods connecting the centers of the two labyrinths are also shown in Figure 2 (Han and Che, 2018).

2. LITERATURE ON TPMS BASED HEAT EXCHANGERS

In general, all minimal surfaces have one significant property that makes them intriguing to study; symmetry. Karcher and Polthier (1996) highlighted that a minimal surface that has a straight-line boundary can be rotated by 180°along the straight line to form a bigger minimal surface. TPMSs have an additional property of translational symmetry in three independent directions, meaning that one can generate an infinite TPMS by simply translating a section of the TPMS in the three directions. For this reason, TPMSs are sometimes called Infinite Periodic Minimal Surfaces (IPMSs).

There are several ways to construct TPMS. The authors use the equations mentioned in Table 1 (Michielsen and Kole, 2003; von Schnering and Nesper, 1991; Wohlgemuth et al., 2001) to generate implicit surfaces. This method is the most widely used in the literature because of its simplicity and ease of implementation.

Table 2 shows the literature (Al-Ketan et al., 2020; Femmer et al., 2015; W. Li et al., 2020; Passos, 2019) on use of TPMS for heat exchange applications. Existing literatures only discuss the three surfaces shown in Figure 2. Among the common P, D, and G TPMSs, D surface has been shown to have the best thermal-hydraulic performance, even better than conventional HX designs in some cases. Apart from the ones listed in Table 2, there are other similar works (Kim and Yoo, 2020; Peng et al., 2019; Reynolds, 2020) that conclude that Schwarz-D TPMS has the best HX implementation due to its high area density.

3. THERMAL HYDRAULIC CHARACTERIZATION OF TPMS HX

Triply periodic minimal surfaces can be divided into balanced and unbalanced structures based on how they divide the R3 space. Balanced TPMSs have an additional property which enables them to separate the R3 space into two congruent domains. This property is of particular interest for fluid-to-fluid heat transfer applications. The authors aim to show a heat transfer and hydraulic performance comparison among several balanced TPMS structures. In order to maintain a common performance metric among the geometries considered, it was made sure that each TPMS unit-cell geometry design had the same hydraulic diameter D_h of $\sim 3.8 - 3.9$ mm. The hydraulic diameters were taken as average of 4 times wetted area by wetted perimeter across 10 different cross-sectional planes along the unit-cell flow direction.

Table 1: Level set approximation functions for common TPMS

TPMS Name	Level set function
P	cos(X) + cos(Y) + cos(Z) = 0
G	sin(X).cos(Y) + sin(Y).cos(Z) + sin(z).cos(X) = 0
D	cos(X).cos(Y).cos(Z) + sin(X).sin(Y).cos(Z) + sin(X).cos(Y).sin(Z) + cos(X).sin(Y).sin(Z) = 0
S	cos(2X).sin(Y).cos(Z) + cos(X).cos(2Y).sin(Z) + sin(X).cos(Y).cos(2Z) = 0
C(Y)	-cos(X).cos(Y).cos(Z) - sin(X).sin(Y).sin(Z) + sin(2X).sin(Y) + sin(2Y).sin(Z) + sin(X).sin(2Z) + sin(2X).cos(Z) + cos(X).sin(2Y) + cos(Y).sin(2Z) = 0
C(±Y)	-2.cos(X).cos(Y).cos(Z) + sin(2X).sin(Y) + sin(X).sin(2Z) + sin(2Y).sin(Z) = 0

Table 2: Literature on TPMS heat exchange applications

Reference	Method(s)	TPMS	Fluids (Hot/Cold)	Additional Information	Results
Femmer et al. (2015)	Expt. (Nu) & CFD (ΔP)	P, D, G & I-WP	Water/ Water	• $5 \times 5 \times 5$ unit cells • $10 \times 10 \times 10$ mm • Liquid polymer resin • $t_W = 0.4\ mm$	• $Nu_{TPMS} > Nu_{plateHX} > Nu_{tubeHX}$ • $Nu_D > Nu_{I-WP} > Nu_G > Nu_P$ for flow above 12 mL/min • $\Delta P_{I-WP} > \Delta P_D > \Delta P_G > \Delta P_P > \Delta P_{tubeHX}$ • $Nu/(Pr^{\frac{1}{3}}f)$ of all TPMS except P better than tubeHX • D TPMS showed better efficiency even at high flow rates
Passos (2019)	CFD	P, D, & G	Air/ Water	• $12 \times 12 \times 12$ mm unit cell • Laminar study (Re< 150)	• Unsteady laminar at Re>150 for D and at Re>75 for P and G • Preferred flow lanes were formed at high Re for P and D • D and G produced higher wall heat flux due to better fluid mixing • D TPMS showed best thermal-hydraulic performance
Al-Ketan et al. (2020)	CFD	D & G (sheet and solid)	Airside only	• TPMS heat sinks • Forced convection • $Re = 4080 - 65000$ • Input load 50W to 500W	• Schwarz-D structure produced 33% higher heat transfer characteristics than Gyroid structure
W. Li et al. (2020)	CFD	D & G	sCO₂/ sCO₂	• $D_h = 1.6\ mm$ • $t_w = 0.7\ mm$ • $5 \times 1 \times 1$ unit cells	• D structure produced high Turbulent Kinetic Energy regions with increasing heat transfer • 30-80% higher heat transfer than PCHX • 50-100% higher friction loss than PCHX • 16-120% higher Nu for a given pumping power

The unit-cell dimensions were also fixed at 15mm × 15mm × 15mm. Since each TPMS geometry differs in its topology, maintaining a fixed hydraulic diameter and dimension meant that each geometry had different wall thickness t_w. Table 3 shows the unit-cell geometries of the four TPMS considered along with their geometric dimensions. For this study the effect of wall thickness was considered negligible when compared to the effect of heat transfer area on the wall thermal resistance. Figure 3 shows the four TPMS unit-cell geometries with the two fluid domains. For the computational analysis, HX designs with 4×4×4 unit-cells of respective TPMS were considered.

3.1 CFD Model Definition
Conjugate heat transfer and fluid flow Computational Fluid Dynamics (CFD) were conducted for each TPMS HX design with 4×4×4 unit-cells. Each TPMS unit-cell geometry was meshed in the *Ansys® Academic Research Mechanical, Release 20.2* (2020) environment using constant size tetrahedral elements with inflation layers to capture the boundary layers. CFD grid uncertainty was resolved by performing a grid convergence study using the Grid Convergence Index method (ASME, 2009; Roache, 1997). Since the unit-cell geometries contained a lot of face details, meshing was done only for 1 unit-cell of each TPMS and then manipulated in *Ansys® Academic Research*

Fluent, Release 20.2 (2020) to merge and create a 4×4×4 unit-cell HX design before performing the CFD analysis. Thermal-hydraulic characterization simulations were conducted for laminar, steady state flow through the TPMS HX geometries. It was assumed that there were no external forces, energy sources or gravitational effects. Water was used as both hot fluid (@ 308.15 K) and cold fluid (@ 278.15 K) for this study. Polynomial curve fits as functions of temperature and pressure were developed from NIST REFPROP (Lemmon et al., 2018), and were utilized for thermophysical properties of water used in the analyses. The convergence criteria were set to 1E-05 for continuity and momentum, and 1E-06 for energy.

Table 3: Geometric details of balanced TPMS geometries considered

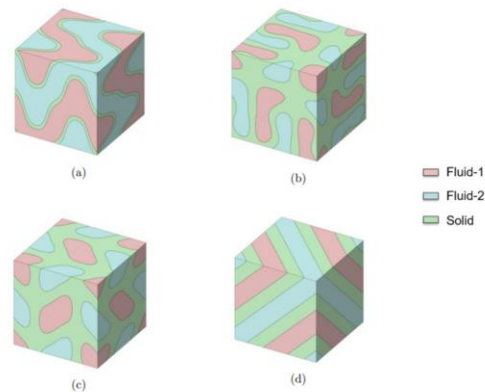| Geometry	Area Density [cm²/cm³]	Hydraulic Diameter [mm]	Wall Thickness [mm]	Image
FK-S	17.98	3.81	0.45	
FK-C(Y)	14.61	3.76	1.00	
FK-C(±Y)	13.64	3.92	1.60	
S-D	11.35	3.92	2.10	

Figure 3: TPMS Unit-cell geometries with fluid domains: (a) Fischer-Koch S [FKS]; (b) Fischer-Koch C(Y) [FK-C(Y)]; (b) Fischer-Koch C(±Y) [FKC(±Y)]; (d) Schwarz-D [S-D]

3.2 CFD Model Definition
Grid independence study was conducted for the four unit-cell TPMS geometries shown in Figure 4. It shows the Grid Convergence Index (GCI) (ASME, 2009; Roache, 1997) for hot side pressure drop and HTC. It can be seen that the GCI is less than 10% for all four TPMS geometries when the mesh size is 0.3 mm.

3.3 TPMS HX Thermal-Hydraulic Performance Evaluation
Next, thermal-hydraulic performance of the selected four TPMS based HXs were evaluated using CFD. Each unit-cell geometry was translated and combined in *Ansys® Academic Research Fluent, Release 20.2* (2020) to form a 4×4×4 cube HX geometry as shown in Figure 5. Adiabatic no-slip wall boundary conditions were assumed for the

external walls. Hot water was inlet at 308.15 K and the cold water was inlet at 278.15 K in counter flow arrangement as shown in Figure 5. 10 different CFD simulations were conducted for each TPMS HX geometry with 10 different inlet Reynolds numbers between 10 and 150. Both fluids were maintained at the same inlet Reynolds number in each simulation for simplicity.
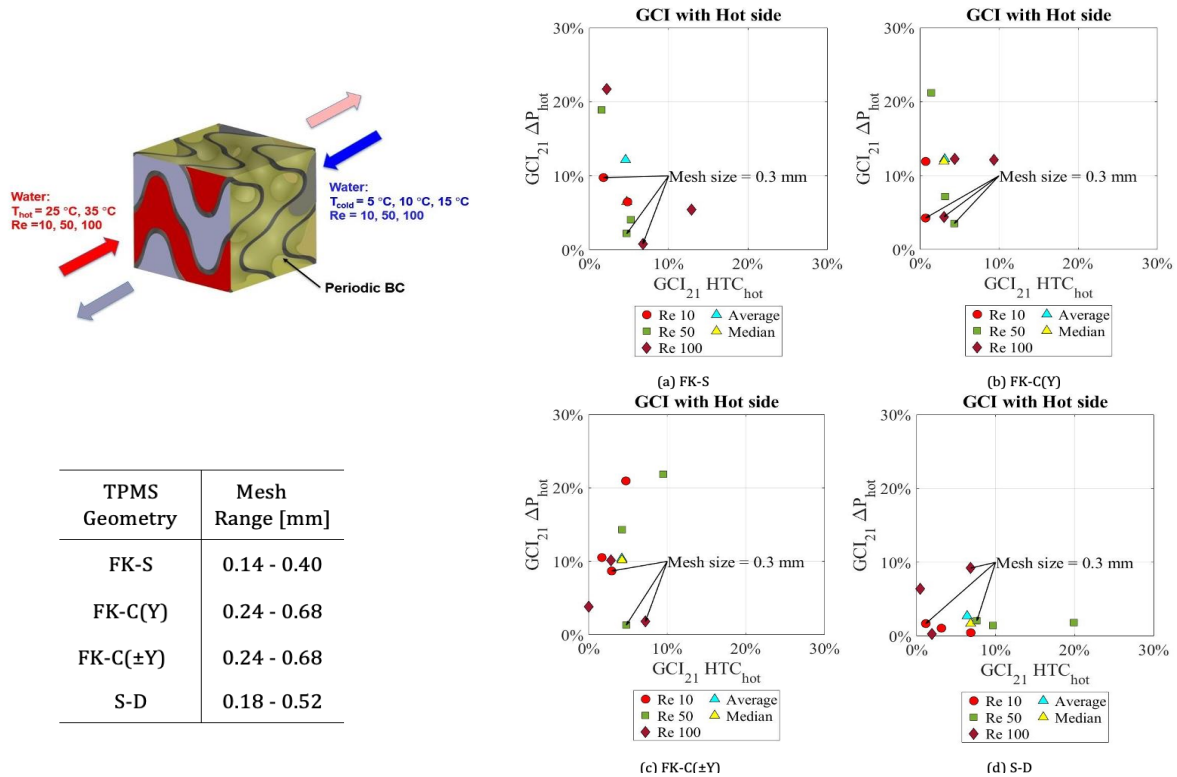

TPMS Geometry	Mesh Range [mm]
FK-S	0.14 - 0.40
FK-C(Y)	0.24 - 0.68
FK-C(±Y)	0.24 - 0.68
S-D	0.18 - 0.52

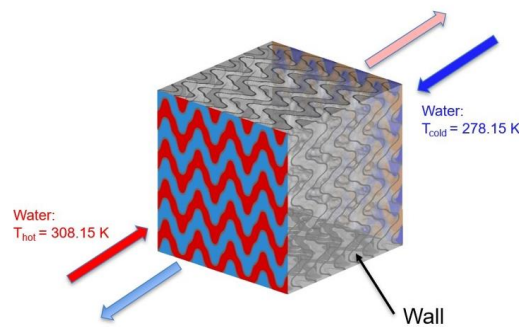**Figure 4:** Grid convergence study on TPMS unit-cells

Figure 5: 4×4×4 FK-S unit-cell TPMS HX geometry with boundary conditions

3.4 Data Reduction

The important equations for data reduction are listed in this section. Friction factors f_D were determined using Darcy-Weisbach equation, given in equation (1), with a correction factor K, given in equation (2), for constant cross-sectional area assumption.

$$f_D = \frac{2 \cdot \Delta P \cdot D_h}{K \cdot \bar{\rho} \cdot \bar{v}^2 \cdot L} \tag{1}$$

$$K = \frac{V}{\bar{A}_{cs} \cdot L} \tag{2}$$

where D_h is the hydraulic diameter of the fluid domain, $\bar{\rho}$ is the volume averaged density of the fluid, $\bar{v}$ is the volume averaged velocity of the fluid, V is the fluid volume, L is the characteristic length of the model, and $\bar{A}_{cs}$ is the average cross-sectional area of the domain. Heat transfer coefficients h_{fl} for both fluids were reduced using UA-LMTD method. Average wall temperatures from CFD, measured near the fluid inlets and outlets were used for the method. Equations (3) – (6) explain the procedure where $\dot{V}$ is the volume flow rate of the fluids, C_p is the specific heat capacity for individual fluid streams at various locations given by subscripts $i, o, h,$ and c, indicating inlet, outlet, hot, and cold, respectively. Finally, a surface "goodness" factor for the heat transfer surface was calculated as a Performance Evaluation Criteria (PEC) (Webb, 1994). PEC for the three Fischer-Koch TPMS HX geometries were calculated in comparison with that of the Schwarz-D TPMS geometry using the equation (7).

$$\dot{Q}_{h/c} = \dot{V}_{h/c} \times \rho_{h/c} \times abs\left(C_{p,h/c,i}T_{h/c,i} - C_{p,h/c,o}T_{h/c,o}\right) \tag{3}$$

$$\Delta T_{LM,h} = \frac{\left(T_{h,i} - T_{wall,h,i}\right) - \left(T_{h,o} - T_{wall,c,i}\right)}{ln\left(\left(T_{h,i} - T_{wall,h,i}\right)/\left(T_{h,o} - T_{wall,c,i}\right)\right)} \tag{4}$$

$$\Delta T_{LM,c} = \frac{\left(T_{wall,h,i} - T_{c,o}\right) - \left(T_{wall,c,i} - T_{c,i}\right)}{ln\left(\left(T_{wall,h,i} - T_{c,o}\right)/\left(T_{wall,c,i} - T_{c,i}\right)\right)} \tag{5}$$

$$h_{fl,h/c} = \frac{\dot{Q}_{h/c}}{A_{HT}\Delta T_{LM,h/c}} \tag{6}$$

$$PEC = \frac{Nu/Nu_{S-D}}{\sqrt[3]{f/f_{S-D}}} \tag{7}$$

4. RESULTS AND DISCUSSIONS

Thermal-hydraulic results from the four TPMS HX geometries are shown in Figure 6 and Figure 7. Figure 6 shows that the three uncharted TPMS HX geometries out-perform the Schwarz-D TPMS structure. The Fischer-Koch S TPMS HX achieved 178% to 356% higher heat transfer when compared to Schwarz-D HX while the C(Y) TPMS HX achieved 35% to 78% higher heat transfer and the C(±Y) achieved 23% to 43% higher heat transfer. In terms of pressure drops across the TPMS HX geometries, C(Y) and C(±Y) HX geometries exhibited values similar to that of the Schwarz-D HX geometry. However, the F-K S TPMS HX showed ~30% lower pressure drops than the Schwarz-D HX. Figure 7 shows the comparison of non-dimensional thermal-hydraulic performances of the four TPMS HX geometries. FK-S showed 4-5 times higher Nusselt numbers (Nu) while FK-C(Y) showed 1.8 times higher Nu and FK-C(±Y) showed 1.5 times higher Nu than the Schwarz-D HX. All four TPMS HX geometries showed very similar friction factor f_D values which is interesting when looking at the pressure drop values. Friction factors of FK-S HX geometry show comparable values with other geometries, which could be attributed to its relatively larger surface area as it is evident from Table 3. In addition, a performance evaluation criteria (PEC) was calculated for the three Fischer-Koch TPMS HX geometries to quantitatively determine the improvements in the thermal-hydraulic performance when compared to the Schwarz-D HX. Figure 8 shows the PEC values at different inlet Reynolds numbers for the three Fischer-Koch TPMS HXs. Since the four TPMS HX geometries had very similar f_D values for all flow rates, the PEC values showed a trend that was like the Nu as seen in Figure 8. It can be concluded that the FK-S TPMS HX showed significantly better thermal-hydraulic performance than the other three TPMS HX geometries considered in the study. The other two Fischer-Koch TPMS HX geometries also showed relatively better thermal-hydraulic performance than the Schwarz-D TPMS HX. Thus, for a given hydraulic diameter, these uncommon TPMS HX geometries show better fluid flow characteristics with significant improvement to the heat transfer performance when compared to the Schwarz-D TPMS HX. It is also interesting to note that the PEC of the TPMS HX geometries scales with the available area which is in line with results from Femmer et al. (2015).

Once it was determined that the uncommon TPMS HX geometries exhibited better thermal-hydraulic performance than the Schwarz-D surface, a separate set of CFD simulations were conducted on the Fischer-Koch S TPMS HX to characterize its thermal-hydraulic performance based on heat transfer and friction factor laws. Three different inlet Reynolds numbers and three different inlet temperatures for hot water side were considered for the study. Similarly,

three different inlet Reynolds numbers and two different inlet temperatures were considered for the cold-water side. Overall, 54 different CFD simulations were conducted in all combinations of inlet Reynolds numbers and inlet temperatures of the fluids. Table 4 lists the temperatures and Reynolds numbers considered for the study.
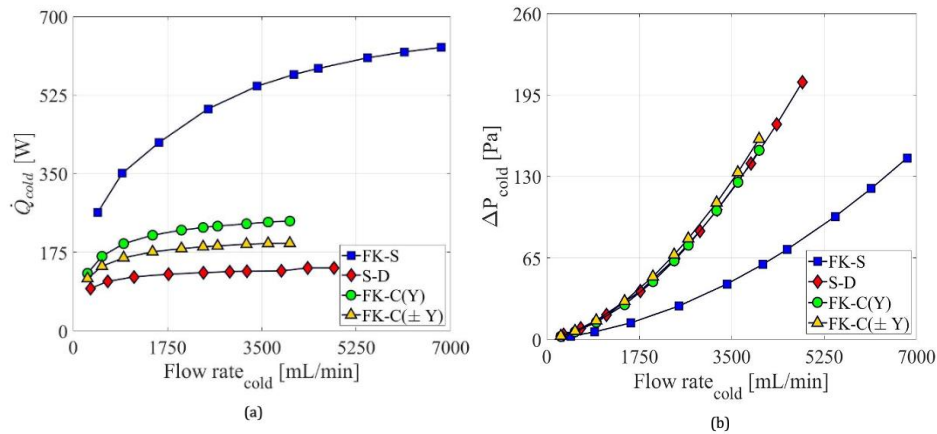
Figure 6: TPMS HX thermal-hydraulic performance comparison: (a) Total heat transferred Vs. flow rate; (b) Pressure drops Vs. flow rate
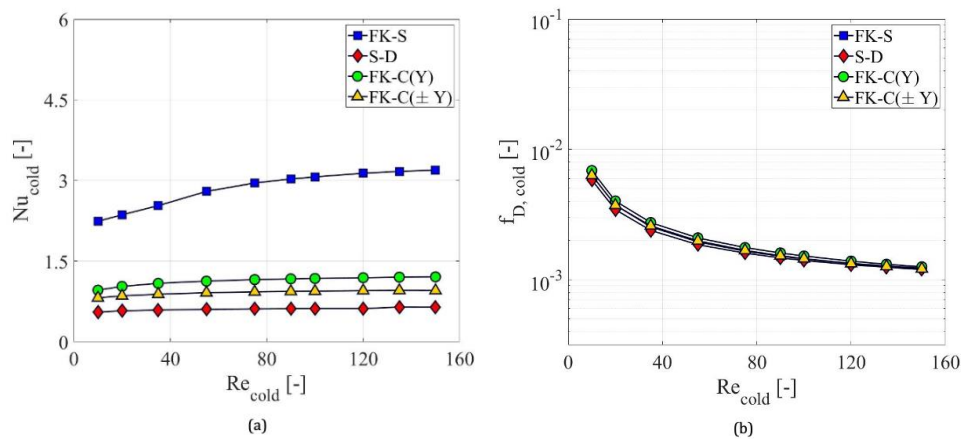
Figure 7: TPMS HX thermal-hydraulic performance comparison: (a) Nusselt number Vs. inlet Reynolds number; (b) Friction factor Vs. inlet Reynolds number
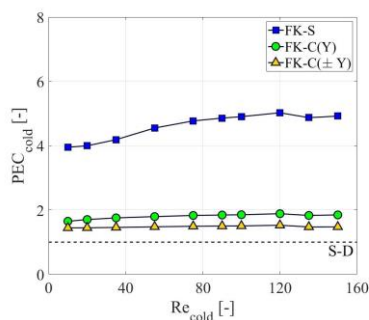
Figure 8: PEC for the Fischer-Koch TPMS HX geometries

Nusselt number results from the CFD simulations were correlated by the generalized heat transfer power law given in the form of equation (8) and the friction factor results from CFD were correlated to inlet Reynolds number (Re) in the form of equation (9).

$$Nu = A \times Re^B \times Pr^C \tag{8}$$

$$f_D = D \times Re^E \tag{9}$$

Parameters A, B, C, D, and E were all determined by performing regression fit of the non-dimensional fluid properties. Equation (10) and equation (11) highlight the determined parameter values. Subsequently, values from the correlations were verified with the results from CFD and the verification plots are shown in Figure 9. Similar correlations for the thermal-hydraulic characteristics of the other two Fischer-Koch TPMS HX geometries could be developed and are planned for future work.

$$Nu = (1.2052) \times R^{(0.1228)} \times P^{(0.1261)} \tag{10}$$

$$f_D = (0.01988) \times R^{(-0.5586)} \tag{11}$$

Table 4: Fluid inlet conditions used for the characterization study

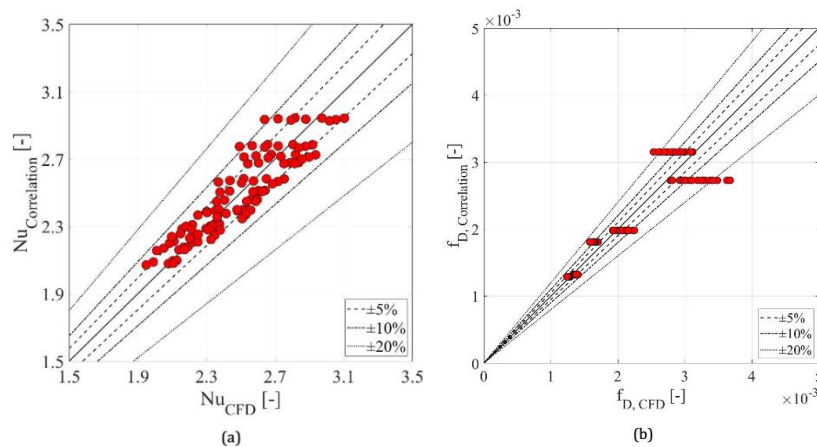| Re_{hot} [-]	$T_{in,hot}$ [K]	Re_{cold} [-]	$T_{in,cold}$ [K]
35	308.15	27	280.65
62	338.15	73	295.65
128	368.15	134	

(a)　　　　　　　　　(b)

Figure 9: FK-S TPMS correlations verification: (a) Nu_{CFD} Vs. $Nu_{correlation}$; (b) $f_{D,CFD}$ Vs. $f_{D,correlation}$

5. CONCLUSIONS

Based on literature it is clear that the TPMS geometries showed great potential for HX applications as they had compact structure and smooth continuous flexures. It has been revealed that Schwarz-D TPMS HX design can outperform compact HX designs like printed circuit HX. However, the complexity in the analysis and fabrication of TPMS structures has been limiting the research efforts to the most common TPMS surfaces. In this research, few understudied TPMS structures were explored for heat exchanger applications and the performance enhancement over Schwarz-D TPMS structure were highlighted. The effect of unit-cell wall thickness on the pressure drop performance of TPMS HX geometries might be significant and warrants a separate study in the future. In addition, thermal-hydraulic characterization of one of the uncommon TPMSs (FK-S) based HX was performed to determine heat transfer and pressure drop correlations. Similar characterization can be performed for the other two TPMS geometries considered in the study. The TPMS HX designs considered in this study are currently being fabricated through additive manufacturing. As a next step in this research, CFD models developed for the TPMS HXs will be validated against experimental results. With the research on TPMS structures gaining traction day by day, the results from this research should serve as motivation to explore other uncommon TPMS structures and that they can provide better results than the more popular Schwarz-P, Schwarz-D, and Gyroid TPMS structures.

REFERENCES

Al-Ketan, O., Ali, M., Khalil, M., Rowshan, R., Khan, K. A., & Abu Al-Rub, R. K. (2020). Forced Convection Computational Fluid Dynamics Analysis of Architected and Three-Dimensional Printable Heat Sinks Based on Triply Periodic Minimal Surfaces. *Journal of Thermal Science and Engineering Applications*, *13*(2). https://doi.org/10.1115/1.4047385

Ansys® Academic Research Fluent, Release 20.2 (R20.2). (2020). [Computer software]. Ansys Inc.

Ansys® Academic Research Mechanical, Release 20.2 (R20.2). (2020). [Computer software]. Ansys Inc.

ASME. (2009). *Standard for Verification and Validation in Computational Fluid Dynamics and Heat Transfer* (ASME V&V 20-2009). American Society of Mechanical Engineers, New York, New York, USA.

Ekade, P., & Krishnan, S. (2019). Fluid flow and heat transfer characteristics of octet truss lattice geometry. *International Journal of Thermal Sciences*, *137*, 253–261. https://doi.org/10.1016/j.ijthermalsci.2018.11.031

Enerdata. (2021, October 5). *World Energy Consumption Statistics | Enerdata* [Data analysis]. EnerData. https://yearbook.enerdata.net/total-energy/world-consumption-statistics.html

Femmer, T., Kuehne, A. J. C., & Wessling, M. (2015). Estimation of the structure dependent performance of 3-D rapid prototyped membranes. *Chemical Engineering Journal*, *273*, 438–445. https://doi.org/10.1016/j.cej.2015.03.029

Han, L., & Che, S. (2018). An Overview of Materials with Triply Periodic Minimal Surfaces and Related Geometry: From Biological Structures to Self-Assembled Systems. *Advanced Materials*, *30*(17), 1705708. https://doi.org/10.1002/adma.201705708

Hyde, S., Blum, Z., Landh, T., Lidin, S., Ninham, B. W., Andersson, S., & Larsson, K. (1996). *The Language of Shape: The Role of Curvature in Condensed Matter: Physics, Chemistry and Biology*. Elsevier.

Karcher, H., & Polthier, K. (1996). Construction of Triply Periodic Minimal Surfaces. *Philosophical Transactions: Mathematical, Physical and Engineering Sciences*, *354*(1715), 2077–2104.

Kim, J., & Yoo, D.-J. (2020). 3D printed compact heat exchangers with mathematically defined core structures. *Journal of Computational Design and Engineering*, *7*(4), 527–550. https://doi.org/10.1093/jcde/qwaa032

Lemmon, E. W., Bell, and I. H., Huber, M. L., & McLinden, M. O. (2018). *NIST Standard Reference Database 23: Reference Fluid Thermodynamic and Transport Properties-REFPROP, Version 10.0, National Institute of Standards and Technology*. https://doi.org/10.18434/T4/1502528

Li, Q., Flamant, G., Yuan, X., Neveu, P., & Luo, L. (2011). Compact heat exchangers: A review and future applications for a new generation of high temperature solar receivers. *Renewable and Sustainable Energy Reviews*, *15*(9), 4855–4875. https://doi.org/10.1016/j.rser.2011.07.066

Li, W., Yu, G., & Yu, Z. (2020). Bioinspired heat exchangers based on triply periodic minimal surfaces for supercritical CO2 cycles. *Applied Thermal Engineering*, *179*, 115686. https://doi.org/10.1016/j.applthermaleng.2020.115686

Lu, W., Zhao, C. Y., & Tassou, S. A. (2006). Thermal analysis on metal-foam filled heat exchangers. Part I: Metal-foam filled pipes. *International Journal of Heat and Mass Transfer*, *49*(15), 2751–2761. https://doi.org/10.1016/j.ijheatmasstransfer.2005.12.012

Mahjoob, S., & Vafai, K. (2008). A synthesis of fluid and thermal transport models for metal foam heat exchangers. *International Journal of Heat and Mass Transfer*, *51*(15), 3701–3711. https://doi.org/10.1016/j.ijheatmasstransfer.2007.12.012

Maloney, K. J., Fink, K. D., Schaedler, T. A., Kolodziejska, J. A., Jacobsen, A. J., & Roper, C. S. (2012). Multifunctional heat exchangers derived from three-dimensional micro-lattice structures. *International Journal of Heat and Mass Transfer*, *55*(9), 2486–2493. https://doi.org/10.1016/j.ijheatmasstransfer.2012.01.011

Meeks, W., & Pérez, J. (2012). *A Survey on Classical Minimal Surface Theory*. American Mathematical Soc.

Michielsen, K., & Kole, J. S. (2003). Photonic band gaps in materials with triply periodic surfaces and related tubular structures. *Physical Review B*, *68*(11), 115107. https://doi.org/10.1103/PhysRevB.68.115107

Motherway, B. (2020). Energy Efficiency 2020. *Energy Efficiency*, 105.

Passos, A. G. P. (2019). *Laminar flow and heat transfer in triply periodic minimal surfaces* [Master's Thesis, Instituto Superior Técnico]. https://fenix.tecnico.ulisboa.pt/downloadFile/1126295043836646/ThesisAndrePassos.pdf

Pelanconi, M., Zavattoni, S., Cornolti, L., Puragliesi, R., Arrivabeni, E., Ferrari, L., Gianella, S., Barbato, M., & Ortona, A. (2021). Application of Ceramic Lattice Structures to Design Compact, High Temperature Heat Exchangers: Material and Architecture Selection. *Materials*. https://doi.org/10.3390/ma14123225

Peng, H., Gao, F., & Hu, W. (2019). *DESIGN, MODELING AND CHARACTERIZATION OF TRIPLY PERIODIC MINIMAL SURFACE HEAT EXCHANGERS WITH ADDITIVE MANUFACTURING* (https://utw10945.utweb.utexas.edu/2019-table-contents). *30*, 13. https://www.sffsymposium.org/.

Reynolds, B. W. (2020). *Simulation of flow and heat transfer in 3D printable triply periodic minimal surface heat exchangers*. https://doi.org/10.26021/11611

Roache, P. J. (1997). QUANTIFICATION OF UNCERTAINTY IN COMPUTATIONAL FLUID DYNAMICS. *Annual Review of Fluid Mechanics*, *29*(1), 123–160. https://doi.org/10.1146/annurev.fluid.29.1.123

Schoen, A. H. (1970). *Infinite Periodic Minimal Surfaces Without Self-Intersections* (Technical Note NASA RN D-5541; p. 92). Cambridge, Massachusetts. https://citeseerx.ist.psu.edu/viewdoc/download?doi=10.1.1.115.3277&rep=rep1&type=pdf

Schwarz, H. A. (1972). *Gesammelte mathematische Abhandlungen*. American Mathematical Soc.

von Schnering, H. G., & Nesper, R. (1991). Nodal surfaces of Fourier series: Fundamental invariants of structured matter. *Zeitschrift Für Physik B Condensed Matter*, *83*(3), 407–412. https://doi.org/10.1007/BF01313411

Webb, R. L. (1994). *Principles of Enhanced Heat Transfer*. Wiley.

Wohlgemuth, M., Yufa, N., Hoffman, J., & Thomas, E. L. (2001). Triply Periodic Bicontinuous Cubic Microdomain Morphologies by Symmetries. *Macromolecules*, *34*(17), 6083–6089. https://doi.org/10.1021/ma0019499